Development 138, 3043-3054 (2011) doi:10.1242/dev.060731
© 2011. Published by The Company of Biologists Ltd

Spatial, temporal and molecular hierarchies in the link between death, delamination and dorsal closure

Sonia Muliyil, Pritesh Krishnakumar and Maithreyi Narasimha*

SUMMARY

Dead cells in most epithelia are eliminated by cell extrusion. Here, we explore whether cell delamination in the amnioserosa, a seemingly stochastic event that results in the extrusion of a small fraction of cells and known to provide a force for dorsal closure, is contingent upon the receipt of an apoptotic signal. Through the analysis of mutant combinations and the profiling of apoptotic signals in situ, we establish spatial, temporal and molecular hierarchies in the link between death and delamination. We show that although an apoptotic signal is necessary and sufficient to provide cell-autonomous instructions for delamination, its induction during natural delamination occurs downstream of mitochondrial fragmentation. We further show that apoptotic regulators can influence both delamination and dorsal closure cell non-autonomously, presumably by influencing tissue mechanics. The spatial heterogeneities in delamination frequency and mitochondrial morphology suggest that mechanical stresses may underlie the activation of the apoptotic cascade through their influence on mitochondrial dynamics. Our results document for the first time the temporal propagation of an apoptotic signal in the context of cell behaviours that accomplish morphogenesis during development. They highlight the importance of mitochondrial dynamics and tissue mechanics in its regulation. Together, they provide novel insights into how apoptotic signals can be deployed to pattern tissues.

KEY WORDS: Apoptosis, Caspases, Cell mechanics, Mitochondrial dynamics, Epithelial morphogenesis

INTRODUCTION

The sculpting of tissues and organs during morphogenesis relies on the spatiotemporal coordination of cell behaviours that include shape changes, migration, proliferation and death. A challenge at the interface of development and cell biology is to find 'molecular explanations for morphology' (Wieschaus, 1996). It is also recognised that tissue morphology is governed by forces and physical principles (Lecuit and Lenne, 2007). Although genetic screens have identified molecules that mediate morphogenesis, how they influence cell behaviours and contribute to the forces that pattern tissues is only beginning to be understood. In addition, how multiple cell behaviours within a tissue and contributions from multiple tissues are coordinated at molecular, cellular and tissue length scales to result in complex morphogenetic movements remains unclear.

In the work we describe here, we explore the utility and necessity of apoptosis in patterning dorsal closure, a complex morphogenetic movement of *Drosophila* embryogenesis. This movement accomplishes the closure of the dorsal surface of the embryo by the epidermis. It is facilitated by the contraction of the ellipse-shaped amnioserosa to which the epidermis is attached and the concerted movement of the leading edge of the epidermis. The former is achieved by apical constriction of the amnioserosa cells. The latter is driven by progressive elongation of lateral epidermal cells, initiated in the leading edge (Jacinto et al., 2002; Kiehart et al., 2000; Narasimha and Brown, 2004; Scuderi and Letsou, 2005). Their coordination ensures that closure spreads inwards from the poles/canthi of the ellipse, a process called zippering, to result in the fusion of the epidermal edges in the dorsal midline. This process is inherently asymmetric and is initiated earlier and progresses faster at the anterior canthus (Jacinto et al., 2000; Kiehart et al., 2000) (see Fig. 1A). Large-scale laser ablation studies have revealed that the contributions of the two tissues to the forces that drive dorsal closure are finely balanced at the interface between the epidermis and the amnioserosa (Hutson et al., 2003). The amnioserosa degenerates at the end of closure by apoptosis triggered nearly synchronously by an ecdysteroid pulse (Hartenstein and Jan, 1992; Wang et al., 2008).

Contraction of the amnioserosa during closure is achieved by apical constriction that exhibits spatial and temporal heterogeneities. One such heterogeneity is cell delamination, the seemingly stochastic, rapid apical constriction of cells that culminates in their extrusion from the layer (Fig. 1B). Their number [between 10 and 30% (Kiehart et al., 2000)] and position is variable and unpredictable. Extruded cells are engulfed by hemocytes. This behaviour is thought to contribute to up to one-third of the force generated in the amnioserosa for dorsal closure and exhibits a preferential occurrence at the anterior canthus. Its suppression by caspase inhibition has led to the suggestion that 'apoptosis' triggers delamination (Toyama et al., 2008). Although cell extrusion/delamination has been reported to follow the induction of apoptosis (Rosenblatt et al., 2001), caspase activation, a common downstream effector of apoptotic signals, has also been demonstrated to have 'non-apoptotic' patterning roles (Geisbrecht and Montell, 2004; Williams et al., 2006). Thus, whether apoptosis is the cause or consequence of cell delamination in the amnioserosa and whether caspase activation is triggered by the induction of apoptosis in delaminating cells is unresolved. Furthermore, the possibility that an apoptotic signal influences both cell delamination and degeneration in the amnioserosa suggests that the same signal may be deployed stochastically and collectively within

Department of Biological Sciences, Tata Institute of Fundamental Research, Colaba, Mumbai 400005, India.

*Author for correspondence (maithreyi@tifr.res.in)

Accepted 28 April 2011

the same tissue to pattern morphogenesis. The conserved molecular machinery and the biochemical understanding of the canonical apoptotic cascade in *Drosophila*, combined with the ease of genetic manipulation and the visualisation of cell behaviours, makes dorsal closure an ideal system to address whether, when, where and how an apoptotic signal impinges on the cellular machinery to instruct cell behaviour and tissue patterning (Fig. 1C).

The apoptotic cascade is triggered by the induction of the pro-apoptotic RHG complex [after the *Drosophila* members Reaper, Hid and Grim that can act individually or together (Jiang et al., 1997)] by various extrinsic signals. They promote death by binding the IAPs [inhibitor of apoptosis, the *Drosophila* orthologues are the DIAPs (Hay and Guo, 2006)]. This relieves the inhibition of IAPs on caspases (effector and initiator), the activation of which mediates apoptosis through specific proteolytic cleavage of substrates (Wang et al., 1999). Induction of apoptosis is also associated with the disruption of both structural and chemical integrity of the mitochondrial network (Hay and Guo, 2006; Suen et al., 2008). Mitochondrial fragmentation can activate caspases through both Cytochrome C-dependent and -independent mechanisms (Abdelwahid et al., 2007; Goyal et al., 2007; Krieser and White, 2009; Sheridan et al., 2008). During *Drosophila* apoptosis, the dynamin related protein Drp1, which acts upstream of caspase activation and downstream of the RHG proteins mediates mitochondrial fragmentation (Fig. 1D) (Abdelwahid et al., 2007; Goyal et al., 2007) while the phospholipase MitoPLD promotes mitochondrial fusion (Choi et al., 2006). How regulators of mitochondrial morphology influence cell behaviour, and whether they function through the apoptotic cascade or independently of it, remains unclear.

In this work, we specifically address whether an apoptotic signal triggers death and subsequent extrusion or whether stochastic changes in cells, as, for example, loss of contact or the stresses they experience, trigger the activation of the apoptotic cascade. In addition, we ask whether death is accomplished through distinct modes during delamination and degeneration. We use genetic perturbations in different classes of pro- and anti-apoptotic molecules and regulators of mitochondrial dynamics (Fig. 1E,F) singly and in combination to examine their utility and necessity for morphogenesis in the amnioserosa. Our results pave the way towards uncovering the complex interplay between stresses, mitochondrial dynamics, apoptosis and cell behaviour.

MATERIALS AND METHODS

Drosophila stocks

The following stocks were used: Canton S (‘wildtype’); c381Gal4 (‘AS::’; for amnioserosa expression; Bloomington Stock Center); armGal4 (‘arm::’; for ubiquitous expression, from J.-P. Vincent, NIMR, London, UK); enGal4 (‘en::’; for epidermal expression, e16E from A. H. Brand, Gurdon Institute, Cambridge, UK); Ubi DECadhGFP (‘ECadhGFP’; from T. Uemura, Kyoto University, Japan) and UAS-αcateninGFP [both to mark apical membranes (Oda and Tsukita, 1999)]; UAS-mitoGFP (to label mitochondria); UAS-actin5CGFP (to label expressing cells), both from Bloomington; and UAS-CD8::PARP-Venus [to detect ‘caspase activity’ (Williams et al., 2006)]. The following stocks were used to perturb the apoptotic cascade: UAS-rpr.C (‘UAS-rpr’, reaper overexpression), UAS-p35.H (UAS-p35) and *hid* ^{05014} (‘*hid*’ amorph), all from Bloomington Stock Center; UAS-hid [*hid* overexpression (Goyal et al., 2007)]; UAS-C [‘UAS-ban’; bantam overexpression (Brennecke et al., 2003)]; UAS-DIAP1 (Hay and Guo, 2006); *drp1*^{2} [‘*drp*’ mutant (Goyal et al., 2007)]; EY11457 (‘*MitoPLD*’ mutant; A. K. Mishra and V. Sriram, personal communication, Bloomington Stock Center); UAS-MitoPLD RNAi (VDRC); and *Dp(2;1)JS13* [drp overexpression (Rikhy et al., 2007)].

The following genotypes (identified unambiguously through the use of GFP-marked balancers) were analysed in the experiments mentioned below. For live imaging (ubiquitous expression), (1) w;UAS-αcateninGFP, armGal4/+;+/+;+/+, (2) w;UAS-αcateninGFP, armGal4/+;UAS-ban/+;+/+, (3) w;UAS-αcateninGFP, armGal4/UAS-p35;+/+;+/+, (4) w;UAS-αcateninGFP, armGal4/UAS-DIAP1;+/+;+/+, (5) w;UAS-αcateninGFP, armGal4/CyO;*hid*/*hid*;+/+ and (6) w;UAS-αcateninGFP, armGal4/UAS-rpr;+/+;+/+. For live imaging (amnioserosa expression), (1) w;ECadh GFP/+;+/+;c381Gal4/+, (2) w;ECadh GFP/+;UAS-ban/+;c381Gal4/+, (3) w;UAS-Actin5C GFP/UAS-p35;+/+;c381Gal4/+, (4) w;UAS-Actin5C GFP/UAS-hid;+/+;c381Gal4/+ and (5) w;UAS-Actin5C GFP/UAS-rpr;+/+;c381Gal4/+. For live imaging (epidermal expression), (1) w;enGal4 ECadhGFP/+; UAS-Actin5CGFP/+;+/+, (2) w;enGal4 ECadhGFP/+; UAS-ban/+;+/+ and (3) w;enGal4 ECadhGFP/UAS-p35;UAS-Actin5CGFP/+;+/+. For imaging mitochondria, (1) w;enGal4 ECadhGFP/+;UAS-mitoGFP/+;+/+ and (2) w;ECadh GFP/+;UAS-mitoGFP/+;c381Gal4/+. For imaging mitochondrial mutants, (1) w;UAS-αcateninGFP, armGal4/*drp1*;+/+;+/+, (2) w;*Dp(2;1)JS13*/+;UAS-αcateninGFP, armGal4/+;+/+;+/+, (3) w;UAS-αcateninGFP, armGal4/*MitoPLD*;+/+;+/+ and (4) w;UAS-αcatenin GFP, armGal4/UAS-MitoPLD RNAi;+/+;+/+. For epistasis experiments, (1) w;ECadhGFP/*MitoPLD*; UAS-ban/+;c381Gal4/+, (2) w;*MitoPLD*,UAS-p35/UAS-αcateninGFP, armGal4;+/+;+/+, (3) w;ECadhGFP/*MitoPLD*;*hid*/*hid*;+/+, (4) w;EcadhGFP/+;UAS-MitoPLD RNAi, *hid*/*hid;*+/+ and (5) *Dp(2:1)JS13*/+;ECadhGFP/+; *hid*/+;+/+. For immunohistochemistry, (1) w;+/+;UAS-CD8::PARP-Venus/+;c381Gal4/+, (2) w;+/+;UAS-MitoPLD RNAi/+;c381Gal4/+ and (3) w;+/+;UAS-rpr/+;c381Gal4/+.

Embryo collection and immunofluorescence

Collections (at 29°C, except for *hid* overexpression, which was carried out at 18°C) were enriched for stage 13-14 embryos. Whole-mount staining of embryos and thick sections were performed according to the standard procedures (Narasimha and Brown, 2006). The following primary antibodies were used: anti-acetylated tubulin (Sigma, 1:500), FITC conjugated phosphotyrosine (Sigma, 1:500), anti-reaper (Santa Cruz; 1:200), anti-cleaved PARP (Abcam, 1:50) and anti-active Caspase 3 (Epitomics, 1:300). Fluorophore-conjugated secondary antibodies were used at 1:200 dilution. Confocal sections were obtained at 0.3 μm steps on an Olympus Fluoview 1000 microscope. Maximum intensity projections of the entire stack or of apical and basal subsets are presented. Levels of fluorescence intensity were adjusted to include the entire area under the curve. Images were assembled using Adobe Photoshop and composites were assembled in Adobe Illustrator.

Live imaging

Embryos were dechorionated and placed in halocarbon oil 700 (Sigma) on a cover slip and then used for imaging on an Olympus Fluoview 1000 confocal microscope at one to two 3D frames per minute. Imaging of embryos across all genotypes was commenced at identical stages using the anterior progression of the hindgut (green in Fig. 1Ab), the position of the spiracles (black arrows in Fig. 1Ab) and the morphology of the midgut basal to the amnioserosa as temporal coordinates, to the end of closure. Images were processed and assembled in Image J (v1.37) and Adobe Photoshop (v7.2, Adobe Microsystems).

Dorsal closure geometry

Ellipse and cell areas were calculated from outlines delineated by αcatenin/ECadherin GFP manually traced from *z* projected images at each time point using Image J. For the dynamic analysis of cell/ellipse areas, graphs were plotted retrospectively such that t=0 marks the end of closure (area of the ellipse is close to zero) or of completion of delamination (area of the cell is close to zero). In the areas represented in the graphs, this area (A0 in keeping with t=0) is subtracted from areas measured at other time points so as to ensure that the graphs converge at t=0. The areas represented in μm^2 in this case are thus close to the absolute areas. Normalised areas for the same were calculated by dividing area at any time point t with that of t=0. This was carried out to remove any bias arising from individual cell sizes. The cell constriction index (CI) was calculated as the ratio of the size

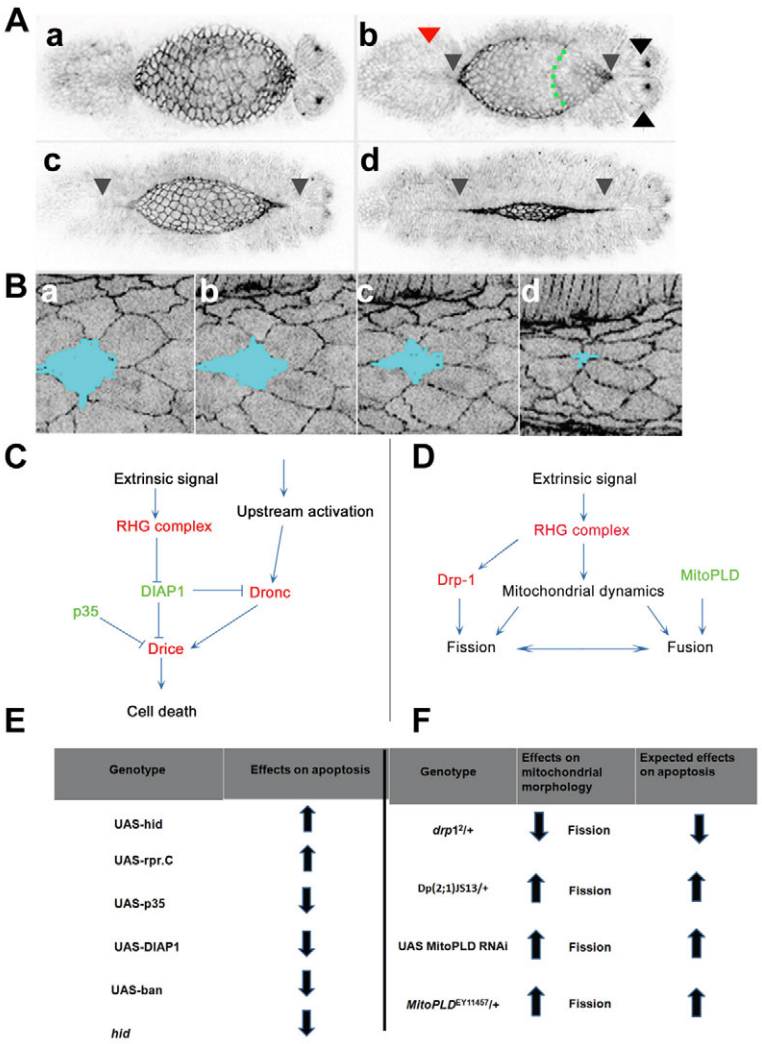

Fig. 1. Dynamics of delamination and dorsal closure and strategies for perturbing apoptosis. (**A**) Stages of a wild-type embryo progressing normally to closure. (a) A mid-stage 13 embryo after the retraction of the germ band to expose the asymmetric ellipse of amnioserosa bound by the taut leading edge. The anterior and posterior poles of the amnioserosa show no zippering. (b) Onset of zippering creates the formation of distinct canthi or poles (grey arrowheads). (c,d) As dorsal closure progresses, the area of the ellipse shrinks and the length of the zippered epidermis increases. The red arrowhead shows the head involution into the interior of the embryo. The hindgut (green) moves antero-dorsally and the posterior spiracles (black arrows) move posterio-medially as dorsal closure progresses providing a coordinate system to stage embryos. (**B**) Progression of a delaminating cell (cyan) over time within the amnioserosa. (**C**) Canonical apoptotic cascade in *Drosophila* showing pro-apoptotic (red) and anti-apoptotic (green) regulators. (**D**) Mitochondrial fragmentation in relation to the apoptotic cascade. (**E**,**F**) Expected effects of perturbations used in this study on apoptosis and mitochondrial dynamics.

of an expressing cell and the average size of its nearest neighbours. When the expressing cell is of the same size as its neighbours, this ratio is close to 1 and tends to be less than 1 when it is constricted relative to its neighbours.

Statistical analysis

The statistical analysis of the significance (*P<0.05, **P<0.01 and ***P<0.001) of differences in phenotype prevalence across genotypes was performed using Microsoft Excel 2003 and Instat graph pad 3.6. Curves and histograms to visualise phenotype penetrance, distribution of different death markers and the dynamic analysis of dorsal closure for all genotypes were plotted using Origin 6.1.

RESULTS

An apoptotic signal provides necessary and sufficient, autonomous and non-autonomous cues for cell delamination

We examined the effects of apoptotic signals on cell behaviour and the spatiotemporal progression of dorsal closure using (1) morphological parameters that are not influenced by the genetic perturbations to enable precise staging (Fig. 1A) (Jacinto and Martin, 2001), (2) genetic perturbations of the apoptotic pathway, through mutants or targeted gene overexpression (Fig. 1E), and (3) real-time 3D confocal microscopy combined with quantitative analysis of cell and tissue morphology dynamics. Cellular delamination in the amnioserosa results in a rosette with the apically constricting delaminating cell at its centre (Fig. 1Ba-Bc) that is eventually extruded (Fig. 1Bd).

To uncover subtle defects in the progress of dorsal closure and the influence on cell behaviour, we imaged embryos of all genotypes from comparable stages (depicted in Fig. 1Ab) to the end of closure and determined: (1) numbers of delaminations, (2) time to complete closure, (3) rates of progression of dorsal closure (the area of the ellipse plotted retrospectively over the last 80 minutes; t=0 marks the end of closure), and (4) rates of apical constriction of individual delaminating cells (t=0 is the time at which the cell disappears from the apical plane of the epithelium).

We first examined perturbations restricted to the amnioserosa (using c381Gal4 with UAS-actinGFP to mark expressing cells or ECadherinGFP to mark all cells). The effects of these perturbations fell into two classes. All anti-apoptotic genotypes showed a complete [bantam overexpression, known to downregulate *Drosophila hid* (Brennecke et al., 2003) and expression of p35, a baculoviral inhibitor of effector caspases (Lannan et al., 2007)] or nearly complete (DIAP1 overexpression) suppression of delamination and delayed closure, evident from the absence of rosettes. Pro-apoptotic perturbations (overexpression of *hid* or *reaper*) significantly increased the number of delaminations and hastened closure (Fig. 2Aa,Ab; see Fig. S1A-E in the

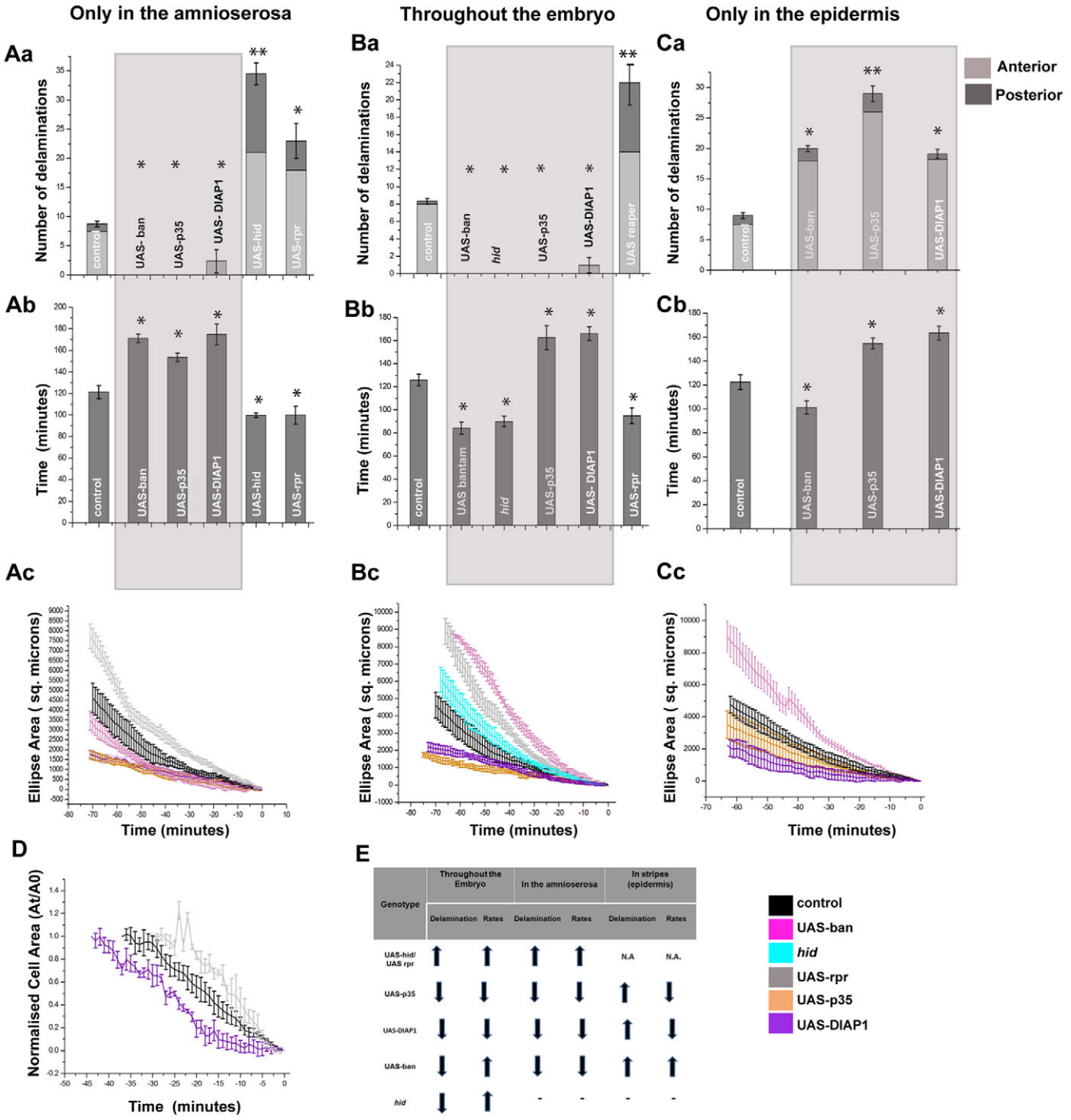

Fig. 2. Effects of apoptotic perturbations on the dynamics of delamination and dorsal closure. (**A-D**) Statistical analysis (mean±s.e.m.; *n*=5 for A-C and *n*=6 for D) of the number of delaminations (Aa,Ba,Ca), the time taken to complete dorsal closure (Ab,Bb,Cb) and the rates of contraction of the ellipse (Ac,Bc,Cc) across apoptotic perturbations tested (genotypes within the bars, colour coded as per key for the curves). Perturbations were driven only in the amnioserosa (Aa-Ac), throughout the embryo (Ba-Bc) and in stripes in epidermis alone (Ca-Cc). The boxed areas (grey) highlight the anti-apoptotic perturbations. Data are mean±s.e.m. **P*<0.05, ***P*<0.01. Dynamics of normalised cell areas (D) in embryos overexpressing *reaper*, DIAP-1 and control (colour coded as per the key and with *t*=0 representing the end of delamination). (**E**) A summary of the above analysis. [Figs S1, S2 in the supplementary material showing snapshots of real time confocal analysis of the dynamics of delamination and dorsal closure (see Fig. S1 in the supplementary material) and the effect on apical constriction (see Fig. S2 in the supplementary material) in the native and perturbed state accompany this figure.]

supplementary material). The analysis of ellipse areas also revealed higher rates of decrease in area in pro-apoptotic perubations and lower rates in anti-apoptotic perturbations compared with control embryos (Fig. 2Ac). A similar trend (higher cell constriction rates with pro-apoptotic perturbations and lower rates with anti-apoptotic perturbations) was observed in the analysis of absolute and

normalised areas of individual delaminating cells (Fig. 2D; see Fig. S2A in the supplementary material). Importantly, the effects of suppression of apoptosis lead us to conclude that an apoptotic signal is not just sufficient but also necessary for delamination and influences both its frequency and its dynamics cell autonomously. Furthermore, they confirm observations that the frequency of delaminations influences the temporal progression of dorsal closure (Toyama et al., 2008).

To exclude the possibility that the effects of suppressing apoptosis are artefacts of high levels of overexpression of inhibitors of Hid or caspases, we analysed an amorphic *hid* mutant. Although delamination events were reduced as expected, closure was unexpectedly hastened (Fig. 2Ba-Bc; see Fig. S1Ha-Hd and Movie 1 in the supplementary material). To understand the basis of this discrepancy, not seen with amnioserosa-specific perturbations, we examined the influence of adjoining tissues, notably also the epidermis using armGal4 (with αcatenin GFP to mark cell membranes) to drive both classes of perturbations. Although all anti-apoptotic perturbations suppressed delamination, their effects on times to and rates of closure separated them into two classes. Whereas *hid* downregulation (mutant and bantam overexpression) resulted in faster closure despite the absence of delaminations (Fig. 2Ba-Bc; see Fig. S1G,H in the supplementary material), inhibiting caspase activity (DIAP1 or p35 overexpression) resulted in slower closure, consistent with the slower rates and the absence of delaminations (Fig. 2Ba,Bb; see Fig. S1I,J in the supplementary material). Induction of apoptosis throughout the embryo by *reaper* overexpression (*hid* overexpression led to widespread death, precluding the analysis of dorsal closure) resulted in a significant increase in delamination events, faster rates and shorter times to closure as expected (Fig. 2Ba-Bc; see Fig. S1K in the supplementary material). These results reveal that apoptotic regulators can influence native dorsal closure through mechanisms other than delamination frequency and dynamics.

To identify the tissue of origin of the differences in rates seen in the anti-apoptotic category, we restricted these perturbations to the epidermis (using enGal4 recombined with ECadherinGFP to mark membranes and UAS-actinGFP to mark the perturbed stripes; see stocks). Epidermal overexpression of bantam reduced the time to dorsal closure, whereas the overexpression of DIAP1 or p35 increased it (Fig. 2Cb,Cc; see Fig. S1M-O in the supplementary material). All three perturbations increased delamination events in the amnioserosa (Fig. 2Ca). These findings suggest that delamination frequency and dorsal closure rates can be uncoupled and uncover cell-autonomous and non-autonomous (originating in the epidermis) influences of apoptosis regulators on both (summarised in Fig. 2E; see also Fig. S2A in the supplementary material).

Mitochondrial fragmentation precedes the activation of the apoptotic cascade in delaminating cells

Our results so far established a role for the apoptotic cascade in influencing cell delamination both qualitatively and quantitatively. To determine when during the course of delamination an apoptotic signal is received, we monitored its propagation en route to cell delamination. Real-time confocal microscopy of embryos expressing a mitochondrially targeted GFP in the entire amnioserosa or in single cells (using enGal4) revealed the progressive fragmentation of mitochondria in delaminating cells. This was evident before visible apical constriction and commenced 30-45 minutes prior to extrusion (Fig. 3A,B,J; see Fig. S3A-C and Movie 2 in the supplementary material). Prior to this, a mixed population of fragmented and tubular mitochondria was observed. This was in contrast to the progressively tubular morphologies observed in non-delaminating cells (Fig. 3A,C; see Movie 3 in the supplementary material). Mitochondria in delaminating cells initially confined apically, dispersed to become progressively basal. By contrast, long mitochondrial tubules remained confined to apical focal planes in non-delaminating cells (see Fig. S3A-F in the supplementary material).

Changes in mitochondrial morphology are considered to be an early indicator of apoptosis operating downstream of a pro-apoptotic signal and upstream of caspase activation (Goyal et al., 2007). We assayed caspase activation in two ways: (1) detecting the cleaved form of the caspase substrate PARP provided in the amnioserosa by the overexpression of a transgene encoding a caspase cleavage site [Gly 201-Ala 240 of human PARP (Williams et al., 2006)] and (2) using an antibody against the active form of Caspase 3. With both reagents, high levels of caspase activity were found in basally localised blobs (larger in size with the transgene than with the antibody) in single cells in the amnioserosa at the end or after delamination and in large numbers of amnioserosa cells beneath the zippered epidermis at the end of dorsal closure (Fig. 3D,E). No caspase activity was detected in non-delaminating cells during early dorsal closure (Fig. 3D,E). To substantiate the temporal order of the initial detection of these changes on account of the differences in the methods of detection, we calculated the cell constriction index (CI; Fig. 3L). Whereas caspase activation was associated with a low index (0.1±0.08; n=12), mitochondrial fragmentation was associated with a constriction index close to one (1±0.2; n=6). We also determined whether and when pro-apoptotic gene expression (detected using antibodies against reaper) is evident. Like caspase activation, reaper expression was evident only in delaminating cells at the end of delamination, in small basally localised blobs in cells of very low index (0.1±0.05, n=10; Fig. 3Fa,Fb,L) and in a larger number of cells beneath the zippered epidermis at the end of closure (Fig. 3Ga,Gb). Thus, although pro-apoptotic gene induction and caspase activation are nearly concomitant late events, mitochondrial fragmentation is the earliest detectable marker of cell delamination (Fig. 3L). Furthermore, the colocalisation statistics of reaper immunoreactivity and caspase activity (52.3% double positive, 17.4% reaper single positive and 29.4% positive for caspase activity alone; n=51) suggest that the two must transiently co-exist in a complex in delaminating cells (Fig. 3H,I). Thus, both delamination and degeneration of the amnioserosa are characterised by the late induction of reaper expression and caspase activation, providing evidence for stochastic and collective modes of activation separated in time and space.

Mitochondrial fragmentation is necessary and sufficient to induce cell delamination

Having identified mitochondrial fragmentation as an early event during delamination, we investigated its necessity for delamination by suppressing mitochondrial fission genetically (in a heterozygous *drp1* mutant, previously shown to be sufficient to induce mitochondrial fusion in *Drosophila* hemocytes; see Fig. S3G and Movie 4 in the supplementary material) (Goyal et al., 2007). This resulted in the suppression of delamination (Fig. 4A,E). By contrast, increasing fission [using a duplication of the *drp1* gene coding region *Dp(2,1)JS13* in the heterozygous state] increased the number of delamination events (Fig. 4B,E; see Fig. S3H in the supplementary material). To address whether the effects were specific to Drp1 or resulted from altered mitochondrial dynamics, we examined the effects of inhibiting fusion through downregulation of MitoPLD. This

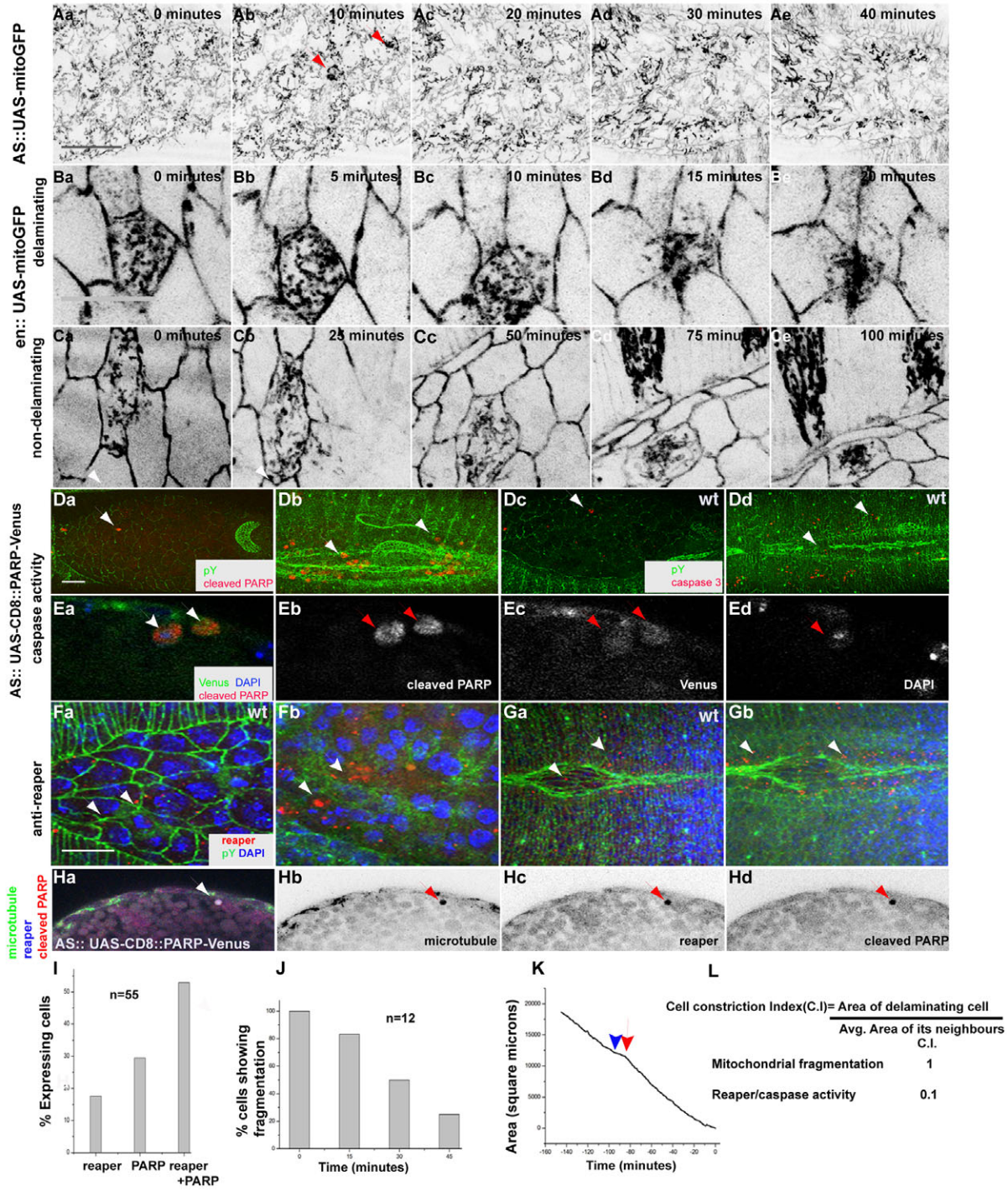

Fig. 3. Propagation of an apoptotic signal during delamination. (**A**) Real-time confocal images of an embryo carrying mitochondrially targeted GFP driven by c381 Gal4 to reveal mitochondrial dynamics and ECadherin GFP to reveal membrane morphology during dorsal closure. Arrowheads (red) indicate a delaminating cell showing mitochondrial fragmentation. (**B**,**C**) Ba-Be and Ca-Ce show mitochondrial dynamics (fragmentation in B and tubular networks in C) in single delaminating (B) and non delaminating (C) cells. (**D**) Visualisation of caspase-mediated cleavage of PARP (red in Da,Db) or caspase activity localisation using the anti-caspase 3 antibody (red in Dc,Dd) in stage-matched embryos. Arrowheads indicate delaminating cells. (**E**) Transverse sections of such embryos (Ea-Ed) showing PARP cleavage (red in Eb, white in Ea) in delaminated and delaminating cells (arrowheads) in which Venus (green in Ea, white in Ec) is diffuse in the cytoplasm. (**F**,**G**) Apical to basal sections of wild-type embryos at stage 14 (Fa,Fb) or at the end dorsal closure (Ga,Gb) showing reaper localisation (red) within a delaminating cell (white arrowheads; phosphotyrosine in green and DAPI in blue). (**H**) Colocalisation of reaper (blue in Ha, black in Hc) and active caspase (red in Ha, black in Hd) in delaminating cells (microtubules are green in Ha, white in Hb). Scale bars: 20 μm. Arrowheads indicate delaminating cells. (**I**) Percentage of cells that are double or single positive for *reaper* and/or caspase activity (*n*=55). (**J**) Frequency distribution of mitochondrial fragmentation with early and progressive fragmentation over time (*n*=12). (**K**) A representative curve of the amnioserosa area dynamics marking the onset of tubular mitochondrial morphology (red arrowhead) in relation to the time of zippering (blue arrowhead). (**L**) Definition and values of cell index associated with mitochondrial fragmentation and detection of *reaper*/caspase activity.

DEVELOPMENT

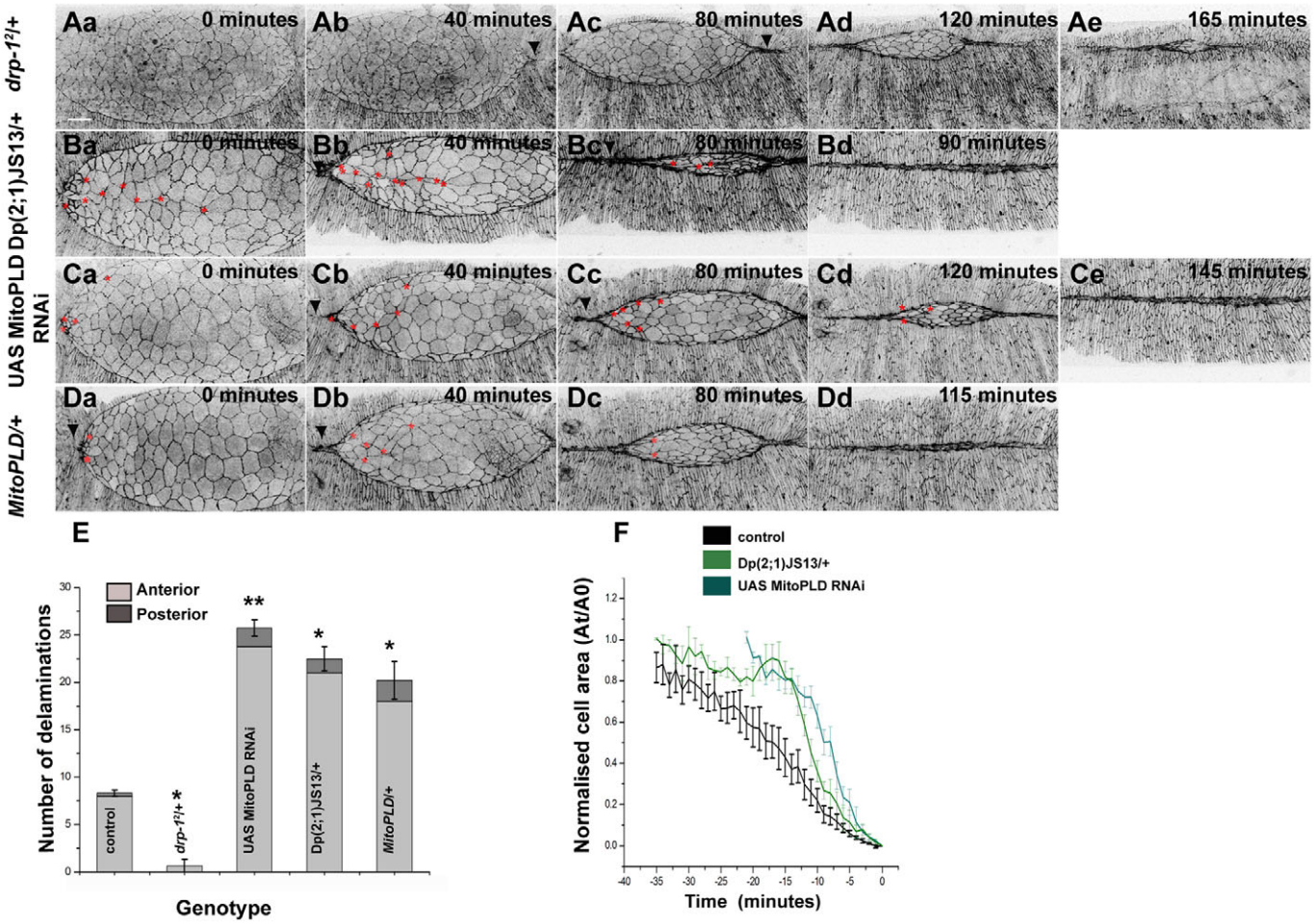

Fig. 4. Role of mitochondrial fragmentation during delamination. (**A-D**) Time lapse confocal images of embryos heterozygous for *drp-1*^{2} (A), the duplication Dp(2;1)JS13 (B) and *MitoPLD* (D), and embryos overexpressing MitoPLD RNAi driven by armadillo Gal4 (C) showing the progress of dorsal closure. Embryos were stage matched using the position of hindgut and posterior spiracles. In this and other images, anterior is towards the left and posterior is towards the right. Asterisks (red) indicate delamination events whereas arrows (black) indicate direction of zippering. (**E**) Mean number of delamination events (±s.e.m.) in the amnioserosa across all classes of mitochondrial perturbations (n=5) recorded from comparable stages (shades of grey indicate anterior and posterior events as per key). *P<0.05, **P<0.01. (**F**) Dynamic analysis of normalised area (mean±s.e.m.; n=6) of delaminating cells in the amnioserosa in various genotypes (colour coded as per key) with t=0 being the end of delamination. Scale bar: 20 μm.

also resulted in a significant increase in the number of delaminations (Fig. 4C-E). Furthermore, both Drp overexpression and MitoPLD downregulation increased the rates of apical constriction of individual delaminating cells, similar to what we observed with pro-apoptotic perturbations (Fig. 4F; see Fig. S2B in the supplementary material). Together, these results establish for the first time, the necessity and sufficiency of mitochondrial fragmentation to accomplish delamination.

Mitochondrial fragmentation functions upstream of pro-apoptotic genes and caspase activation

Mitochondria are involved in cell proliferation, differentiation and death, and can influence metabolism dynamics, Ca^{2+} homeostasis and energy generation within cells (Okamoto and Shaw, 2005; Vander Heiden et al., 2000). Mitochondrial fragmentation can occur downstream of a number of distinct signals, including pro-apoptotic genes (Goyal et al., 2007), caspase activation (Tanner et al., 2010) and in the absence of apoptosis (Varadi et al., 2004; Verstreken et al., 2005). Our analysis suggests the possibility that mitochondrial fragmentation triggers the apoptotic cascade (rather than being induced by it) to induce delamination and death. We performed genetic epistasis experiments in the amnioserosa to test this hypothesis. We first analysed the combined effect of downregulating both Hid (through *bantam* overexpression, which suppressed delamination) and MitoPLD (increased delaminations). We observed a complete suppression of delamination with rates of amnioserosa contraction comparable with control rather than higher than it (Fig. 5A,B; see Fig. S4A in the supplementary material). This suggested that Hid functions downstream of mitochondrial fragmentation to cause delamination. To further validate this suggestion, embryos that were homozygous for the *hid* mutant (reduced delamination) and carried either an extra copy of Drp1 or reduced levels of MitoPLD (both previously shown to increase delamination) were examined. Delamination was suppressed in both backgrounds and closure rates were comparable with embryos that were homozygous for the *hid* mutation (Fig. 5A,B; see Fig. S4C-E in the supplementary material), further substantiating the hypothesis that mitochondrial fragmentation acts upstream of the activation of pro-apoptotic genes.

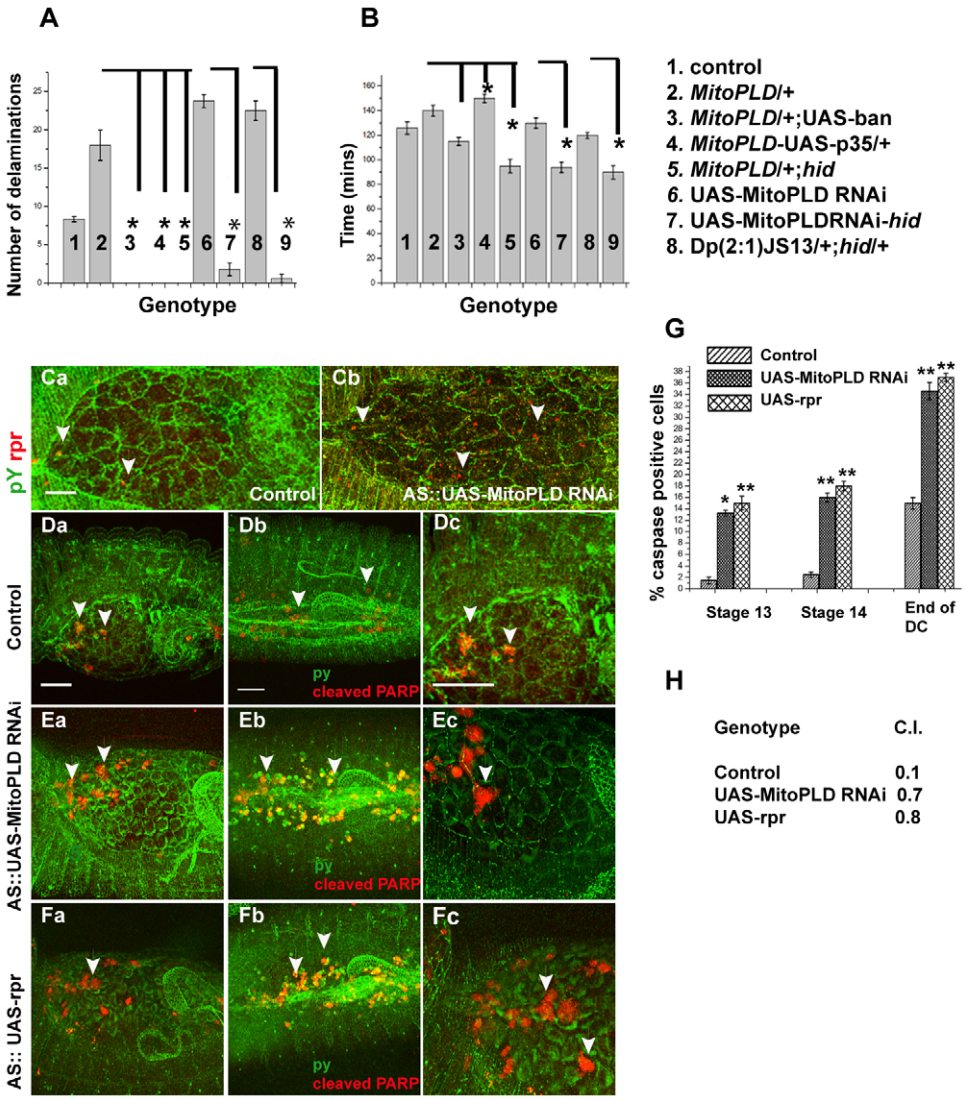

Fig. 5. Mitochondrial changes are upstream of apoptotic signal induction. (**A**) Mean number of delamination events in the amnioserosa in single and double mutant embryos (*n*=5; genotypes numbered as per key) recorded from comparable stages and (**B**) their respective times taken to closure. Data are mean±s.e.m. **P*<0.05, ***P*<0.01. (**C**) Reaper expression (red) in embryos overexpressing MitoPLD RNAi in the amnioserosa alone (Cb) versus control (Ca) counterstained with phosphotyrosine (green) to mark membranes. Arrowheads indicate reaper blobs. (**D-F**) Arrowheads (white) indicate active caspase blobs. Caspase activity (red) in control (D), MitoPLD RNAi (E) and *reaper*-overexpressing embryos (Fa-Fc) counterstained with phosphotyrosine (green). Scale bars: 20 μm. (**G**) Stage-wise detection of caspase-positive cells in control and mutant genotypes as coloured in the key. Data are mean±s.e.m. **P*<0.05, ***P*<0.01. (**H**) Cell index at first detection of caspase activity in all classes of perturbations.

To test the hierarchical relationship between activation of caspases and mitochondrial fragmentation, embryos overexpressing p35 in the amnioserosa in the background of MitoPLD downregulation were analysed. Again, a complete suppression of delamination was observed and ellipse contraction rates were similar to the reduced rates found upon p35 overexpression (Fig. 5A,B; see Fig. S4B in the supplementary material). Taken together, the genetic rescue experiments place mitochondrial fragmentation upstream of stochastic *reaper*/*hid* induction and caspase activation. Furthermore, they suggest that caspase activation is a necessary intermediate in the link between mitochondrial fragmentation and cell delamination.

To test this hierarchy further, we examined whether reaper induction and caspase activation are contingent on mitochondrial fragmentation. MitoPLD downregulation in the amnioserosa resulted in the early (high cell constriction index) upregulation of reaper (Fig. 5Ca,Cb) and caspase activation (Fig. 5D,E,H) with the numbers of such cells highest in older embryos and greater than control embryos at all stages examined (Fig. 5G). Caspase activation was similarly upregulated in embryos overexpressing *reaper* (Fig. 5F-H), suggesting that *reaper* can activate caspases. Together, our results suggest that mitochondrial fragmentation triggers the induction of the RHG complex and through it, caspase activation to instruct delamination. Our results do not exclude the possibility that low, undetectable levels of pro-apoptotic genes and caspase activity in the entire amnioserosa are permissive for mitochondrial fragmentation that, once initiated, results in the marked upregulation of the cascade in single cells. Two further findings lend support to the existence of this third mode of operation of apoptotic regulators. Expression of p35 suppresses the transition from tubular to fragmented mitochondria in some cells, suggesting that caspases may also serve as permissive cues for fragmentation (see Fig. S3I in the supplementary material). Second, downregulation of either *hid* or caspases results in reorganisation of the actin cytoskeleton throughout the amnioserosa (S.M. and M.N., unpublished), implying a requirement for their activation in all cells. Together, our results uncover three modes of operation of an apoptotic cascade in the amnioserosa and suggest the interplay between local and global activation of the same cascade in executing cell delamination.

Spatial heterogeneities in mitochondrial dynamics and delamination frequency

Our examination of delamination frequency revealed a predominance of delamination events (Toyama et al., 2008), pro-apoptotic gene induction and caspase activation in the anterior half

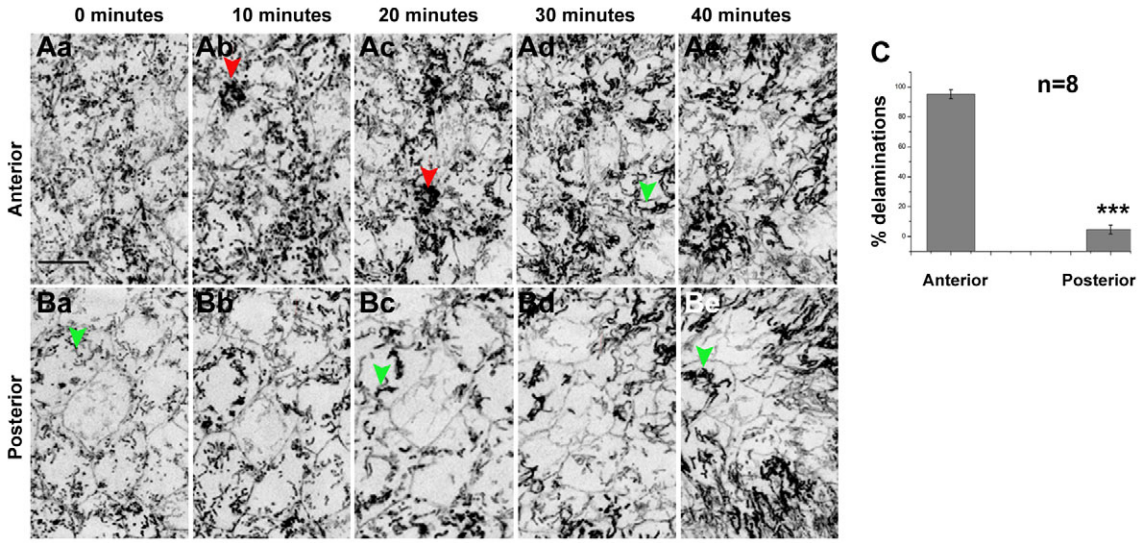

Fig. 6. Spatial heterogeneities associated with delamination and mitochondrial morphology dynamics. (**A**,**B**) Snapshots of anterior (Aa-Ae) and posterior (Ba-Be) halves of the amnioserosa of a wild-type embryo expressing mitochondrially targeted GFP in combination with E-cadherin GFP to mark membranes. Red arrowheads indicate delaminating cells and green arrowheads indicate tubular mitochondria. (**C**) A statistical analysis of the distribution of delaminations in the anterior versus posterior halves of the amnioserosa during native closure. Data are mean±s.e.m. ***P<0.001 Scale bar: 20 μm.

of the amnioserosa, even when genetic perturbations included the entire amnioserosa (Fig. 2Aa-Ca, Fig. 4E, Fig. 5D-F, Fig. 6C). This prompted us to examine the pattern of mitochondrial dynamics in anterior and posterior halves of the amnioserosa. Time lapse confocal microscopy of mitoGFP in combination with ECadherinGFP revealed the temporal progression from a mixed population of fragmented and tubular structures to extremely tubular/hyperfused states towards the end of dorsal closure (Fig. 3A). The detection of tubular states coincided with the initiation of zippering (Fig. 3K). Mitochondria in the posterior half of the amnioserosa became tubular significantly ahead of the anterior cells, which showed a more frequent occurrence of fragmented states associated with delaminating cells (Fig. 6A,B; see Movies 5 and 6 in the supplementary material). This observation provides the first evidence for an early molecular/physiological difference between the two halves of the amnioserosa. We discuss the origin of these heterogeneities and their implications for patterning cell behaviour (see Discussion, Fig. 7C,D).

DISCUSSION

Apoptosis has been shown to signal tissue and organ patterning through mechanisms that are poorly understood at cellular and molecular length scales (Baehrecke, 2002; Benedict et al., 2002; Green and Evan, 2002; Kuranaga et al., 2011; Opferman and Korsmeyer, 2003). ‘Apoptosis’ has also been shown to provide forces for dorsal closure through its influence on delamination in the amnioserosa (Toyama et al., 2008), but how the induction of an apoptotic signal is regulated spatiotemporally, and how it is transduced and translated to accomplish delamination remain poorly understood. We show here that the amnioserosa deploys an apoptotic cascade in two spatiotemporally distinct patterns – stochastic (delamination) and collective (degeneration) – and unequivocally establish the necessity of apoptotic signals for cell delamination. We demonstrate that the cascade is upregulated in delaminating cells by prior, stochastic, mitochondrial fragmentation. We delineate the temporal and molecular hierachies in the apoptotic cascade in the context of cell delamination in an intact animal for the first time and suggest that stresses may pattern its spatiotemporal induction. Finally, we uncover both autonomous and non-autonomous roles for apoptotic regulators that influence cell and tissue mechanics in addition to their influence on delamination (Fig. 7). Together, our results provide several novel insights into the link between death, delamination and dorsal closure, and uncover complexities not previously appreciated (Toyama et al., 2008).

Utility, necessity and autonomy of apoptotic signals for delamination

Our results establish the necessity and utility of apoptotic signals in driving cellular delamination in the amnioserosa and in patterning the spatiotemporal dynamics of closure. They invoke the induction of pro-apoptotic genes and thus go beyond earlier observations (Toyama et al., 2008) that inferred the role of an apoptotic cascade through the effects of caspase suppression. Our results also provide mechanistic insights into the mode of action of the apoptotic cascade by demonstrating cell-autonomous effects of pro-apoptotic genes and caspase activity (DIAP1 overexpression) on the rates of apical constriction. This suggests that apoptotic regulators must regulate cytoskeletal organisation and cell mechanics. A question that arises is whether both classes of regulators function in the linear hierarchy we have delineated or whether functions independent of the apoptotic cascade contribute to their role in driving delamination. Our analysis of the molecular hierarchy shows that caspase activation induced by reaper upregulation is a necessary downstream event. Its late activation in delaminating cells, however, raises the issue of whether it is necessary for apical constriction or just for cell extrusion. Although the complete suppression of delamination by p35 overexpression precludes the analysis of constriction rates, our analysis reveals an absence of rosette patterns that characterise delamination rather than the presence of constricted cells that fail to extrude (see Fig. S1C in the supplementary material). This suggests that caspase activation must also be

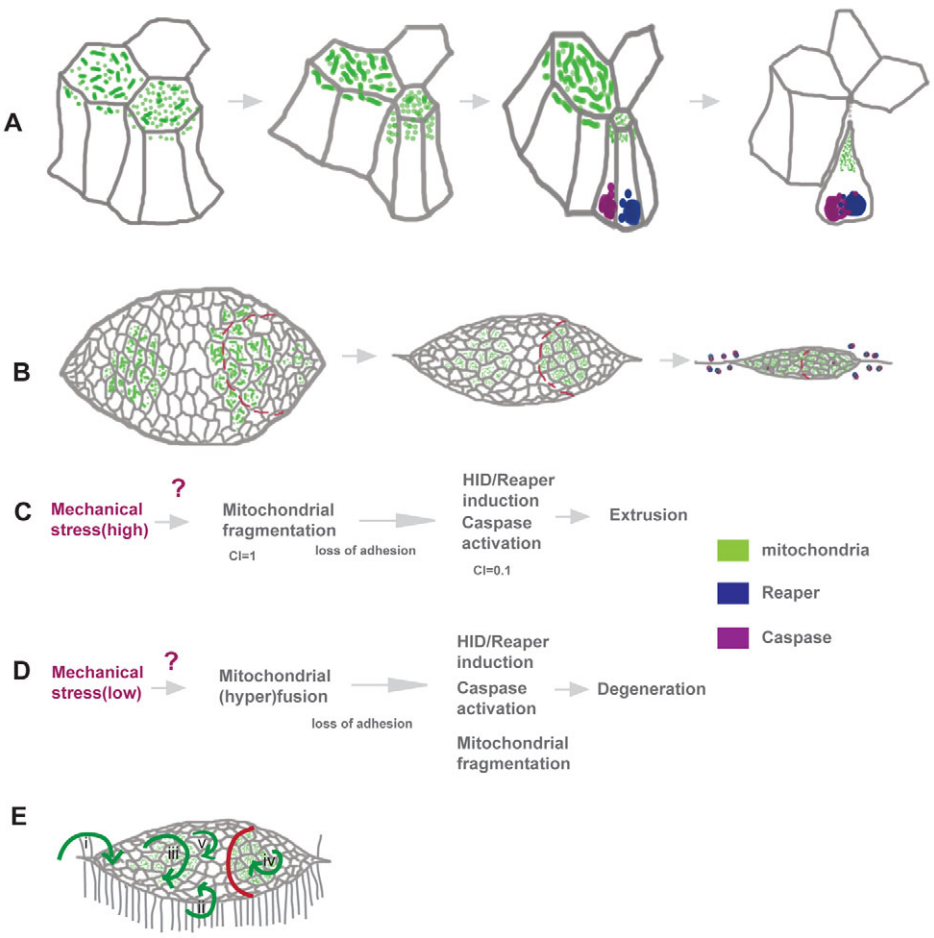

Fig. 7. Hierarchies in the link between death, delamination and dorsal closure. (**A**) A hemi-rosette with the delaminating cell at its centre progressively constricting its apical surface is shown with the sequence of detection of markers and molecules associated with delamination (mitochondria, green; *reaper*, magenta; caspase activity, blue). (**B**) The spatial heterogeneities in mitochondrial morphology dynamics (green) associated with dorsal closure with the anterior end (left) showing more cells with fragmented morphologies and the delayed transition to tubular morphologies compared to the posterior (right). The red line marks the position of the hindgut and the boundary of adhesion anisotropies. Reaper (magenta) and caspase activity (blue) are also shown. (**C**,**D**) A model linking mechanical stresses to stochastic (delamination) and collective (degeneration) cell behaviour through the regulation of mitochondrial morphologies. (**E**) The origin of non-autonomous influences on cell delamination: head involution (i), leading edge of the epidermis (ii), adhesion to yolk cell (iii), adhesion to hindgut (iv) and non-autonomous influences originating within the amnioserosa (v).

necessary for apical constriction. One explanation is that this marked upregulation of the cascade triggers the almost abrupt transition in cell behaviour, characterised by the rapid fall in cell area in a delaminating cell. This is consistent with the higher rates of decrease in cell area with increases in the amounts of caspases/Reaper. Although the phenotypes associated with DIAP1 overexpression also support a role for caspases in cell constriction, caspase-independent functions of DIAP1 have been reported to influence actin organisation in *Drosophila* border cells (Geisbrecht and Montell, 2004). Thus, apoptotic signals must impinge on a distinct set of regulators of the actin cytoskeleton to facilitate apical constriction and tissue contraction. Caspase activation may also regulate adhesion to facilitate extrusion. Indeed, the adherens junction component armadillo/β-catenin is a caspase substrate during cell death in *Drosophila* and mammals (Kessler and Müller, 2009).

Our results also provide evidence for cell non-autonomous regulation of delamination by components of the apoptotic cascade (Fig. 2, Fig. 7E). Further support for this comes from our ongoing observations that caspase inhibition influences actin organisation in the entire amnioserosa (S.M. and M.N., unpublished). We speculate that the influence of low undetectable levels of caspase activation not restricted to delaminating cells, regulates tissue mechanics in the amnioserosa and through it also influences cell delamination. Our results also show that non-autonomous influences on delamination can originate in the epidermis. Uncovering the molecular players that underlie both autonomous and non-autonomous effects of apoptotic signals on cell behaviour will be interesting avenues to pursue.

Molecular hierarchies and spatial heterogeneities in the link between death and delamination

Temporal and epistatic analysis position mitochondrial fragmentation upstream of the induction of pro-apoptotic genes and caspase activation both during delamination and degeneration (Fig. 7A,B). This, to our knowledge, is the first time that the sequence of propagation of an apoptotic signal has been elucidated in the context of cell behaviour in vivo. Mitochondrial fragmentation is thus the earliest indicator we have so far of the cellular commitment to delamination. Other studies have placed mitochondrial fragmentation downstream of the pro-apoptotic genes *reaper* and *hid* (Abdelwahid et al., 2007; Goyal et al., 2007; Suen et al., 2008). What, if not the pro-apoptotic genes, then triggers mitochondrial fragmentation in the amnioserosa? Two recent reports have documented the ability of chemical and radiation injuries to trigger changes in mitochondrial morphology and lead to the induction of apoptosis (Dagda et al., 2008; van der Bliek, 2009). An attractive candidate for the trigger in the amnioserosa, consistent with the spatial heterogeneities in delamination frequency and mitochondrial morphology we observe, is mechanical stress (Fig. 7). Two sets of observations support this. First, not all cells that overexpress pro-apoptotic genes delaminate and the anterior predominance of such events is maintained (Fig. 2Aa,Ba,Ca, Fig. 4E). This suggests that although an apoptotic signal is necessary, it must cooperate with other permissive signals to accomplish delamination. Second, our studies of native dorsal closure uncover spatial heterogeneities in mitochondrial morphology. Two features characterise this

heterogeneity: (1) the early abundance of cells with predominantly fragmented mitochondria in the anterior AS and (2) their delayed transition to tubular/hyperfused morphologies prior to degeneration compared with the posterior. It has been suggested in a different context that low levels of chemical stress can induce hyperfusion as a means of countering stress (through optimisation of mitochondrial ATP production), whereas higher magnitudes of stress lead to fragmentation and apoptosis (Tondera et al., 2009; van der Bliek, 2009). A similar reasoning (with the substitution of chemical stresses by mechanical stresses) might underlie the spatial heterogeneities in delamination frequency. Specifically, high magnitudes of stress locally (from head involution) might be responsible for increased mitochondrial fragmentation and subsequent delamination, whereas prolonged lower levels of stresses (from the leading edge) may drive hyperfusion and subsequent degeneration of the amnioserosa. Adhesion anisotropies resulting from differences in the substrate (yolk anteriorly and hindgut posteriorly) could additionally contribute to the force anisotropies between the anterior and posterior amnioserosa (Fig. 7C,D).

‘Apoptotic forces’ driving dorsal closure

Taken together, our results reveal that apoptotic regulators contribute multiple forces to dorsal closure. In the amnioserosa, they act locally to drive delamination but also globally to maintain tissue tension. We attribute the latter to the low levels of caspase activation and pro-apoptotic gene induction. This, we argue, provides a permissive environment for mitochondrial fragmentation and the subsequent marked upregulation of the cascade in delaminating cells. Additionally, they contribute to forces generated in the epidermis. This is best inferred from anti-apoptotic perturbations. In *hid* mutants, the rates of dorsal closure are higher despite the absence of delaminations in the amnioserosa. Conversely, delamination in the amnioserosa is ‘upregulated’ when either caspases or *hid* is downregulated in the epidermis, but their effects on closure rates are different. These non-autonomous effects must reflect the feedback regulation of forces generated in the epidermis and in the amnioserosa (Fig. 7D). That multiple forces contribute to dorsal closure and can feedback regulate each other has been long appreciated (Kiehart et al., 2000; Peralta et al., 2007). Our studies identify apoptotic signals as crucial regulators of the balance of forces that drive dorsal closure. Uncovering the basis for feedback regulation and the force hierarchies that lend dorsal closure resilience will be interesting. A recent study reported on a novel, non-apoptotic role for an epidermal caspase, caspase 8: its effect on interleukin signalling resulted in the recapitulation of a wound healing response when deleted in the skin (Lee et al., 2009). In light of the above observations, it is interesting that in our analysis of dorsal closure, which recapitulates wound closure, some perturbations that suppress apoptosis also resulted in accelerated closure.

Conclusions

Our explorations demonstrate the primacy of mitochondrial fragmentation in the induction of apoptotic signalling and uncover the complex relationships between death signals, delamination and dorsal closure. Furthermore, they illustrate how an apoptotic signal is deployed multiple times in the same tissue to accomplish heterogeneity in cell behaviour and have helped identify some of the cellular properties they modulate. Understanding the triggers for mitochondrial fragmentation and the precise outcomes and mechanisms of apoptotic signals on cell biological attributes of delaminating cells will be interesting avenues to explore.

Acknowledgements

We thank Drs Steve Cohen, Bruce Hay, Yasushi Hiromi, Hiroki Oda, Veronica Rodrigues, Apurva Sarin, Herman Steller and Tadashi Uemura; the Bloomington Stock Center; and the Developmental Studies Hybridoma Bank for fly stocks and antibodies. We especially thank Dr V. Sriram for sharing unpublished reagents and Drs Ullas Kolthur, Veronica Rodrigues, Apurva Sarin, G. V. Shivashankar and V. Sriram for discussions and comments on the manuscript, and lab members for support. We also thank Dr Thomas Lecuit and anonymous reviewers for constructive criticisms that improved the manuscript. We thank TIFR (M.N.) and a CSIR JRF Fellowship (P.K.) for support. M.N. dedicates this paper to the memory of Veronica Rodrigues.

Competing interests statement

The authors declare no competing financial interests.

Supplementary material

Supplementary material for this article is available at
http://dev.biologists.org/lookup/suppl/doi:10.1242/dev.060731/-/DC1

References

Abdelwahid, E., Yokokura, T., Krieser, R. J., Balasundaram, S., Fowle, W. H. and White, K. (2007). Mitochondrial disruption in Drosophila apoptosis. *Dev. Cell* **12**, 793-806.

Baehrecke, E. H. (2002). How death shapes life during development. *Nat. Rev. Mol. Cell Biol.* **3**, 779-787.

Benedict, C. A., Norris, P. S. and Ware, C. F. (2002). To kill or be killed: viral evasion of apoptosis. *Nat. Immunol.* **3**, 1013-1018.

Brennecke, J., Hipfner, D. R., Stark, A., Russell, R. B. and Cohen, S. M. (2003). bantam encodes a developmentally regulated microRNA that controls cell proliferation and regulates the proapoptotic gene hid in Drosophila. *Cell* **113**, 25-36.

Choi, S.-Y., Huang, P., Jenkins, G. M., Chan, D. C., Schiller, J. and Frohman, M. A. (2006). A common lipid links Mfn-mediated mitochondrial fusion and SNARE-regulated exocytosis. *Nat. Cell Biol.* **8**, 1255-1262.

Dagda, R. K., Merrill, R. A., Cribbs, J. T., Chen, Y., Hell, J. W., Usachev, Y. M. and Strack, S. (2008). The spinocerebellar ataxia 12 gene product and protein phosphatase 2A regulatory subunit Bbeta2 antagonizes neuronal survival by promoting mitochondrial fission. *J. Biol. Chem.* **283**, 36241-36248.

Geisbrecht, E. R. and Montell, D. J. (2004). A role for Drosophila IAP1-mediated caspase inhibition in Rac-dependent cell migration. *Cell* **118**, 111-125.

Goyal, G., Fell, B., Sarin, A., Youle, R. J. and Sriram, V. (2007). Role of mitochondrial remodeling in programmed cell death in Drosophila melanogaster. *Dev. Cell* **12**, 807-816.

Green, D. R. and Evan, G. I. (2002). A matter of life and death. *Cancer Cell* **1**, 19-30.

Hartenstein, V. and Jan, Y. N. (1992). Studying Drosophila embryogenesis with P-lacZ enhancer trap lines. *Dev. Genes Evol.* **201**, 194-220.

Hay, B. A. and Guo, M. (2006). Caspase-dependent cell death in Drosophila. *Annu. Rev. Cell Dev. Biol.* **22**, 623-650.

Hutson, M. S., Tokutake, Y., Chang, M.-S., Bloor, J. W., Venakides, S., Kiehart, D. P. and Edwards, G. S. (2003). Forces for morphogenesis investigated with laser microsurgery and quantitative modeling. *Science* **300**, 145-149.

Jacinto, A. and Martin, P. (2001). Morphogenesis: unravelling the cell biology of hole closure. *Curr. Biol.* **11**, 705-707.

Jacinto, A., Wood, W., Balayo, T., Turmaine, M., Martinez-Arias, A. and Martin, P. (2000). Dynamic actin-based epithelial adhesion and cell matching during Drosophila dorsal closure. *Curr. Biol.* **10**, 1420-1426.

Jacinto, A., Woolner, S. and Martin, P. (2002). Dynamic analysis of dorsal closure in Drosophila: from genetics to cell biology. *Dev. Cell* **3**, 9-19.

Jiang, C., Baehrecke, E. H. and Thummel, C. S. (1997). Steroid regulated programmed cell death during Drosophila metamorphosis. *Development* **124**, 4673-4683.

Kessler, T. and Müller, H. A. J. (2009). Cleavage of Armadillo/beta-catenin by the caspase DrICE in Drosophila apoptotic epithelial cells. *BMC Dev. Biol.* **9**, 15.

Kiehart, D. P., Galbraith, C. G., Edwards, K. A., Rickoll, W. L. and Montague, R. A. (2000). Multiple forces contribute to cell sheet morphogenesis for dorsal closure in Drosophila. *J. Cell Biol.* **149**, 471-490.

Krieser, R. J. and White, K. (2009). Inside an enigma: do mitochondria contribute to cell death in Drosophila? *Apoptosis* **14**, 961-968.

Kuranaga, E., Matsunuma, T., Kanuka, H., Takemoto, K., Koto, A., Kimura, K. and Miura, M. (2011). Apoptosis controls the speed of looping morphogenesis in Drosophila male terminalia. *Development* **138**, 1493-1499.

Lannan, E., Vandergaast, R. and Friesen, P. D. (2007). Baculovirus caspase inhibitors P49 and P35 block virus-induced apoptosis downstream of effector caspase DrICE activation in Drosophila melanogaster cells. *J. Virol.* **81**, 9319-9330.

Lecuit, T. and Lenne, P. F. (2007). Cell surface mechanics and the control of cell shape, tissue patterns and morphogenesis. *Nat. Rev. Mol. Cell Biol.* **8**, 633-644.

Lee, P., Lee, D. J., Chan, C., Chen, S. W., Ch'en, I. and Jamora, C. (2009). Dynamic expression of epidermal caspase 8 simulates a wound healing response. *Nature* **458**, 519-523.
Narasimha, M. and Brown, N. H. (2004). Novel functions for integrins in epithelial morphogenesis. *Curr. Biol.* **14**, 381-385.
Narasimha, M. and Brown, N. H. (2006). Confocal microscopy of Drosophila embryos. In *Cell Biology: A Laboratory Handbook*, Vol. 3 (ed. J. E. Celis), pp. 77-86. San Diego: Academic Press.
Oda, H. and Tsukita, S. (1999). Dynamic features of adherens junctions during Drosophila embryonic epithelial morphogenesis revealed by a Dalpha-catenin-GFP fusion protein. *Dev. Genes Evol.* **209**, 218-225.
Okamoto, K. and Shaw, J. M. (2005). Mitochondrial morphology and dynamics in yeast and multicellular eukaryotes. *Annu. Rev. Genet.* **39**, 503-536.
Opferman, J. T. and Korsmeyer, S. J. (2003). Apoptosis in the development and maintenance of the immune system. *Nat. Immunol.* **4**, 410-415.
Peralta, X. G., Toyama, Y., Hutson, M. S., Montague, R., Venakides, S., Kiehart, D. P. and Edwards, G. S. (2007). Upregulation of forces and morphogenic asymmetries in dorsal closure during Drosophila development. *Biophys. J.* **92**, 2583-2596.
Rikhy, R., Kamat, S., Ramagiri, S., Sriram, V. and Krishnan, K. S. (2007). Mutations in dynamin-related protein result in gross changes in mitochondrial morphology and affect synaptic vesicle recycling at the Drosophila neuromuscular junction. *Genes Brain Behav.* **6**, 42-53.
Rosenblatt, J., Raff, M. C. and Cramer, L. P. (2001). An epithelial cell destined for apoptosis signals its neighbors to extrude it by an actin- and myosin-dependent mechanism. *Curr. Biol.* **11**, 1847-1857.
Scuderi, A. and Letsou, A. (2005). Amnioserosa is required for dorsal closure in Drosophila. *Dev. Dyn.* **232**, 791-800.
Sheridan, C., Delivani, P., Cullen, S. P. and Martin, S. G. (2008). Bax- or Bak-induced mitochondrial fission can be uncoupled from cytochrome c release. *Mol. Cell* **31**, 570-585.
Suen, D.-F., Norris, K. L. and Youle, R. J. (2008). Mitochondrial dynamics and apoptosis. *Genes Dev.* **22**, 1577-1590.
Tanner, E. A., Blute, T. A., Brachmann, C. B. and McCall, K. (2010). Bcl-2 proteins and autophagy regulate mitochondrial dynamics during programmed cell death in the Drosophila ovary. *Development* **138**, 327-338.
Tondera, D., Grandemange, S., Jourdain, A., Karbowski, M., Mattenberger, Y., Herzig, S., Da Cruz, S., Clerc, P., Raschke, I., Merkwirth, C. et al. (2009). SLP-2 is required for stress-induced mitochondrial hyperfusion. *EMBO J.* **28**, 1589-1600.
Toyama, Y., Peralta, X. G., Wells, A. R., Kiehart, D. P. and Edwards, G. S. (2008). Apoptotic force and tissue dynamics during Drosophila embryogenesis. *Science* **321**, 1683-1686.
van der Bliek, A. M. (2009). Fussy mitochondria fuse in response to stress. *EMBO J.* **28**, 1533-1534.
Vander Heiden, M. G., Chandel, N. S., Li, X. X., Schumacker, P. T., Colombini, M. and Thompson, C. B. (2000). Outer mitochondrial membrane permeability can regulate coupled respiration and cell survival. *Proc. Natl. Acad. Sci. USA* **97**, 4666-4671.
Varadi, A., Johnson-Cadwell, L. I., Cirulli, V., Yoon, Y., Allan, V. J. and Rutter, G. A. (2004). Cytoplasmic dynein regulates the subcellular distribution of mitochondria by controlling the recruitment of the fission factor dynamin-related protein-1. *J. Cell Sci.* **117**, 4389-4400.
Verstreken, P., Ly, C. V., Venken, K. J. T., Koh, T.-W., Zhou, Y. and Bellen, H. J. (2005). Synaptic mitochondria are critical for mobilization of reserve pool vesicles at Drosophila neuromuscular junctions. *Neuron* **47**, 365-378.
Wang, L., Evans, J., Andrews, H. K., Beckstead, R. B., Thummel, C. S. and Bashirullah, A. (2008). A genetic screen identifies new regulators of steroid-triggered programmed cell death in Drosophila. *Genetics* **180**, 269-281.
Wang, S. L., Hawkins, C. J., Yoo, S. J., Muller, H. A. and Hay, B. A. (1999). The Drosophila caspase inhibitor DIAP1 is essential for cell survival and is negatively regulated by HID. *Cell* **98**, 453-463.
Wieschaus, E. F. (1996). Autobiography. In *Les Prix Nobel* 1995 (ed. T. Frängsmyr). Stockholm: Nobel Foundation.
Williams, D. W., Kondo, S., Krzyzanowska, A., Hiromi, Y. and Truman, J. W. (2006). Local caspase activity directs engulfment of dendrites during pruning. *Nat. Neurosci.* **9**, 1234-1236.